Tailored Ultralow Dielectric Permittivity in High-Performance Fluorinated Polyimide Films by Adjusting Nanoporous Characterisitics

ARTICLE *in* THE JOURNAL OF PHYSICAL CHEMISTRY C · NOVEMBER 2012

Impact Factor: 4.77 · DOI: 10.1021/jp305286r

4 AUTHORS, INCLUDING:

Jun-Wei Zha
University of Science and Technology Beijing
83 PUBLICATIONS **1,136** CITATIONS
SEE PROFILE

Zhimin Dang
Tsinghua University
176 PUBLICATIONS **4,019** CITATIONS
SEE PROFILE

THE JOURNAL OF PHYSICAL CHEMISTRY C

Article

pubs.acs.org/JPCC

Tailored Ultralow Dielectric Permittivity in High-Performance Fluorinated Polyimide Films by Adjusting Nanoporous Characterisitics

Jun-Wei Zha,[†] Hong-Juan Jia,[‡] Hai-Yan Wang,[§] and Zhi-Min Dang*[,†,‡]

[†]Department of Polymer Science and Engineering, University of Science and Technology Beijing, Beijing 100083, People's Republic of China

[‡]State Key Laboratory of Chemical Resource Engineering, Beijing University of Chemical Technology, Beijing 100029, People's Republic of China

[§]State Key Laboratory of Gansu Advanced Non-ferrous Metal Materials, Lanzhou University of Technology, Lanzhou 730050, People's Republic of China

ABSTRACT: To acquire advanced nanoporous fluorinated polyimide (F−PI) films with low dielectric permittivity applied in microelectronic fields, as a feasible tactic, the SiO_2/F−PI nanohybrid films were first synthesized to employ an in situ polymerization process by controlling the dispersion of SiO_2 nanoparticles in polymer and the chemical reaction of monomers composed of F−PI. Then, the removal of SiO_2 nanoparticles from the SiO_2/F−PI nanohybrid films by HF acid etching gives rise to the amount of nanopores with a diameter of about 40 nm in the porous F−PI films, which can be confirmed by observing TEM image results. The relationship between the microstructure of the nanoporous F−PI films and the properties, including relative dielectric permittivity, thermal stability, contact angles, and mechanical strength, was discovered. The relative dielectric permittivity of the nanoporous F−PI films was decreased to 2.45 while the films still displayed good mechanical properties and thermal stability. So this type of advanced nanoporous F−PI films brings a very potential application as alternative dielectric layers in the future microelectronic technology.

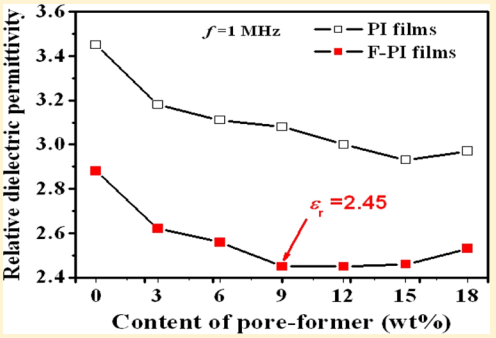

INTRODUCTION

Polyimides (PIs) have many desirable characteristics such as excellent mechanical properties, low relative permittivity, high breakdown field, inertness to solvent, and radiation resistance. They are distinguished from other high performance polymers by the solubility of the poly(amic acid) precursor form, which can be casted into uniform films and quantitatively converted to polyimide. Up to now, PIs have been especially used widely in microelectronic technology as films and adhesives and in membrane industry due to these prior properties. PI films are often used as the interlevel dielectric insulators within large-scale integration current (LSI) in the microelectronic industry due to low relative permittivity in the range 2.9−3.4 and other excellent properties of PI materials.[1−6] The utmost importance for the microelectronic applications is to pursue lower dielectric permittivity and excellent mechanical properties of PI films. For example, as microelectronic packaging materials, low dielectric permittivity materials would minimize cross talk of signal and maximize signal propagation speed in devices. Hence, the development of PI with lower dielectric permittivity has been an interesting focus for researches.[7−10] In recent years, the introduction of fluorinated groups and nanopores into polymers to reduce their dielectric permittivities has been demonstrated.[11−13]

Fluorinated polyimides (F−PI) have received extensive attention due to their low dielectric permittivity, which is an increasing attraction in the new generation microelectronic technology. The following equation, namely, the Clausius−Mosottti equation, gives some routes for how to decrease the dielectric permittivity.[14]

$$\frac{\varepsilon_r - 1}{\varepsilon_r + 2}\frac{M}{\rho} = \frac{N}{3\varepsilon_0}\left(\alpha_e + \alpha_i\frac{\mu^2}{3kT}\right) \quad (1)$$

where ε_r is the relative dielectric permittivity of the material, M and ρ are the molecular weight and density, respectively, N is the Avogadro constant, α_e and α_i are respectively polarizabilities of electrons and the dipole orientation, and μ is the dipole moment. Therefore, the decreases of polarizability and density of materials were considered to be the effective methods for debasing the dielectric permittivity of materials, which was well described by Simpson and Clair.[15] Among the strategies used to reduce the dielectric permittivity of PI are as follows. An incorporation of diamine and dianhydride reactants could minimize the polarizability of PI. The incorporation could also

Received: May 30, 2012
Revised: October 9, 2012
Published: October 23, 2012

   dx.doi.org/10.1021/jp305286r | J. Phys. Chem. C 2012, 116, 23676−23681

impart a high degree of free volume. In addition, an incorporation of fluorine atoms into the molecular structure of the PI was also considered to be a good way. For example, Hougham et al.[7] and Onah et al.[8] mainly are interested in fluorine introduction to polyimide structure in order to decrease dielectric permittivity. They reported that the incorporation of fluorine into polyimide structure has been intensively explored in the past decade and also the increase of fluorine amount has been found to generally reduce the dielectric permittivity and moisture absorption.

The incorporation of air, which has a dielectric permittivity of about 1.0, can decrease the density of materials so that the low relative dielectric permittivity can be reached by means of this simple route. The approaches to preparation of porous PI films include microwave processing[16] and incorporation of foaming agents[17] and hollow microspheres[18,19] were reported in past studies. The size and size distribution of pores are of great importance to the mechanical and dielectric properties of the porous materials. A better control to the size and size distribution of pores in the PI films can probably be achieved through a better method to produce nanopores. And the incorporation of pores in fluorinated polyimides is expected to provide several advantages, including reduced relative dielectric permittivity and excellent mechanical properties. Chen et al. prepared the nanoporous F−PI films with porosity in the range 2−10% and pore size in the range 20−50 nm by employing the reversible addition−fragmentation chain transfer (RAFT)-moderated process. The dielectric permittivity of the nanoporous F−PI films was close to 2.0.[20] In our previous work, ultralow relative dielectric permittivity (ε_r = 2.58) nanohybrid films were obtained by dispersing 3.0 wt % mesoporous silicate (MCM-41) particles with nanosize hollow channels into PI.[21] However, there is a lack of research on the nanoporous F−PI films filled with mesoporous inorganic particles and related thermal behavior and mechanical properties.

In this work, we report on an alternative approach to fabricate the nanoporous fluorinated polyimide films with low relative dielectric permittivity ε_r < 2.5, which is presently the most convenient and simplest method compared with other reports.[22,23] The SiO_2/F−PI nanohybrid films with 2,2-bis[4-(4-aminophenoxy) phenyl] hexafluoropropane (3FEDAM) and 4,4′-(hexafluoroisopropylidene) diphthalic anhydride (6FDA) were successfully synthesized by a wet phase inversion process. Then, the removal of the SiO_2 nanoparticles from the SiO_2/F−PI nanohybrid films by HF acid etching gives rise to the amount of nanopores with a diameter of about 40 nm in F−PI films, which can be confirmed by observing TEM image results. Effects of the nanoporous structure of the F−PI films on relative dielectric permittivity, thermal stability, contact angles, and mechanical strength were discovered. The relative dielectric permittivity of nanoporous F−PI films was decreased to 2.45 while the films still displayed good mechanical properties and thermal stability.

EXPERIMENTAL SECTION

Materials. 4,4′-(Hexafluoroisopropylidene) diphthalic anhydride (6FDA) with a molecular weight of 444 and 2,2-bis[4-(4-aminophenoxy) phenyl] hexafluoropropane (3FEDAM) with a molecular weight of 518 were bought from J&K Scientific. SiO_2 nanoparticles with a diameter of 50 nm were bought from Sibnano Technology Lt. Co. (Beijing, China). *N*,*N*′-dimethylacetamide (DMAc) was obtained from Beijing Chemical Reagent Co. (Beijing, China).

Synthesis of the SiO_2/F−PI Nanohybrid Films and Nanoporous PI Films. The 6FDA and 3FEDAM were heated in a vacuum at 160 and 80 °C for about 6 h before use, respectively. SiO_2 nanoparticles with the surfaces modified by a single organic chain and DMAc were added to a three-necked flask equipped with a mechanical stirrer. Ultrasonic treatment for 1 h was applied to increase the dispersion of SiO_2 nanoparticles. Then, 3FEDAM was added to the flask which cooled in a water bath under a nitrogen atmosphere. After the 3FEDAM had dissolved completely, 6FDA was added and the mixture was stirred for 12 h. The obtained DMAc solution of the SiO_2/fluorinated polyamic acid was coated onto a glass plate. Subsequently, the plates were heated for 1 h at 80, 120, 180, 240, and 300 °C, respectively. The film was then peeled off from the glass plate to obtain the SiO_2/F−PI nanohybrid films. Then, the removal of the SiO_2 nanoparticles from the SiO_2/F−PI nanohybrid films by HF acid etching gives rise to the nanoporous F−PI films. The porosity of the films is due to the amount of SiO_2 nanoparticles (which is also called pore-forming agent variation from 0 to 18 wt %). As a comparison, pure, non-fluorinated PI films were also used to prepare the SiO_2/PI nanohybrid films and subsequently the nanoporous PI films by using the same method.

Characterization. ^{1}H nuclear magnetic resonance (^{1}H NMR) spectra were obtained at 600 MHz using a Bruker AC-80 MHz spectrometer. Fourier transform infrared (FT-IR) spectroscopy measurements were performed using a 60 SXB FT-IR spectrophotometer in the range 0−4500 cm^{-1}. Thermogravimetric analysis (TGA) was performed on a Netzsch TG/DTA in a nitrogen atmosphere at a heating rate of 10 °C/min. Small samples with dimensions of 1 cm^2 area and about 30 μm thickness were cut from sheets and were pasted with silver electrodes on both sides to minimize contact resistance for electrical measurements. The dielectric permittivity of the nanoporous films was measured by Agilent 4294A Impedance Analyzer at various frequencies and temperatures. The contact angles were measured by the contact angle measurement of GS&LP. Transmission electron microscope (TEM) analyses were carried out by using a Hitachi H-800 to characterize the microstructure of the films. The mechanical strength of the prepared films was determined by an almighty material testing machine (Instron, Model 1185).

RESULTS AND DISCUSSION

^{1}H NMR Spectroscopy and FT-IR Measurement. We employed monomers with $-CF_3$, 6FDA, and 3FEDAM to prepare F−PI. The structure of the monomers can be characterized from ^{1}H NMR spectroscopy. Figure 1a and b displays the ^{1}H NMR spectra and molecule structure of 6FDA and 3FEDAM, respectively. In Figure 1a, the aryl protons are represented by peaks at 8.12, 8.03, and 7.89 ppm. We assign the peaks at 3.4 and 3.6 ppm to the protons of the $-NH_2$ units of the 3FEDAM. The FT-IR spectra of the F−PI films are depicted in Figure 1c. When $-CF_3$ is introduced to the polyimide films, a peak attributed to the presence of fluorinated groups has been observed at 1204 cm^{-1}. Furthermore, peaks at 1724 and 1786 cm^{-1} (C═O stretching vibration), 1502 cm^{-1} (N—N stretching vibration), 711 and 823 cm^{-1} (C—O stretching vibration) corresponding to imide structure were observed.[24] These results confirm the successful preparation of the F−PI films in this work.

Microstructure of the Porous F−PI Films. Figure 2a and b displays TEM images of the porous structure of the F−PI

dx.doi.org/10.1021/jp305286r | J. Phys. Chem. C 2012, 116, 23676−23681

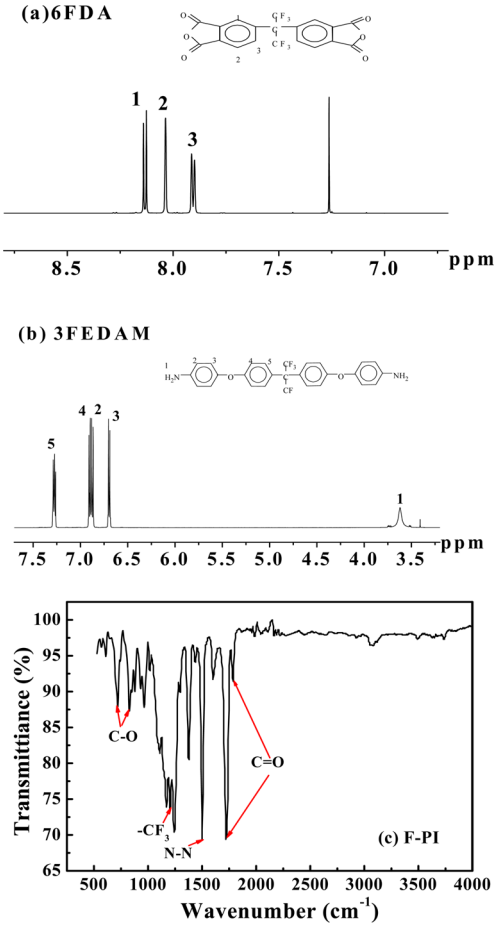

Figure 1. ^{1}H NMR spectra of (a) 6FDA and (b) 3FEDAM and (c) FT-IR spectra of the F−PI film.

films with contents of pore-former (SiO_2 nanoparticle) at 3 and 9 wt %. We observe that the uniform distribution of nanopores with about 50 nm exists in the F−PI films (see the inset in Figure 2a) after the SiO_2 nanoparticles are etched and the nanopores possess a small degree of interconnection. With increasing concentration of SiO_2 nanoparticles, as shown in Figure 2c and d, the pore size in these F−PI films with the contents of pore-former at 12 and 18 wt % have become larger and there is a greater degree of pore interconnection in these films. The results suggest that the differences in size and distribution of nanopores are from the dispersion of SiO_2 nanoparticles. When the content of pore-former is more than 9 wt %, the conglomeration size of SiO_2 nanoparticles increases from 50 nm to more than 100 nm so that the size of pores is increased after the SiO_2 nanoparticles are etched.

Dielectric Properties of the Films. The relative dielectric permittivity of the films was calculated from the measurements of the capacity at 1 MHz and room temperature. The dielectric permittivity could be acquired from the measured capacitance data as follows:

$$\varepsilon_r = Cd/\varepsilon_0 A \quad (2)$$

where C is the capacitance, ε_r is the relative dielectric permittivity, ε_0 is the permittivity of the free space, and d and A are the film thickness and electrode area, respectively. Figure 3a shows the relative dielectric permittivity dependence on the content of pore-former in the porous PI films and F−PI films. It is clear that relative dielectric permittivities of all films decrease gradually with increasing content of pore-former. That is because the dielectric permittivity of air (pores) was only 1.0, which is beneficial to reduce the dielectric permittivity of hybrid films. Compared to pure F−PI film (without pores), the relative dielectric permittivity of the F−PI film with 9 wt % SiO_2 nanoparticle loading is only 2.45, which is decreased by about 15.5% due to the porous presence in the film. Compared to pure PI film, because of the presence of bulky trifluoromethyl groups in 6FDA and 3FEDAM monomer, ε_r of pure F−PI film is decreased by about 15.9%. Furthermore, this result can also be explained due to the formation of a cross-linking network structure, which restricts orientation and relaxation of dipoles.[25] Though the relative dielectric permittivity of the 9 wt % SiO_2 nanoparticle loading F−PI film is low to 2.45, ε_r of the films increases when the content of pore-former is above 12 wt %. This is because the size of pores is so big that they reduce the thickness of the films, which in turn amplifies ε_r of the films. This result confirms the restriction of orientation and relaxation of polar groups by the introduction of fluorinated groups. Figure 3b shows the variation of relative dielectric permittivity on temperature for the pure PI film, pure F−PI film, porous PI film, and porous F−PI film after the 9 wt % SiO_2 nanoparticles are etched. In the low temperature range, polar groups of polymers are difficult to orient and relax under the applied electrical field because of the molecular chain segments in the glassy state. With increasing temperature, the chain segment mobility increases and polar groups start to move in response to the applied electrical field, which increase the orientation of polymer chains so that an increased relative dielectric permittivity is often observed. As seen from Figure 3b, we notice that ε_r of the PI films presents an unstable variation with temperature. Namely, it can be seen that ε_r of the pure PI film and porous PI film display a remarkable increase at about 25 °C. However, ε_r of two kinds of F−PI films have exhibited negligible changes with temperatures. A low (∼2.4) and relatively stable ε_r over a wide temperature range from −50 to 150 °C is realized in our porous F−PI films. For many microelectronic applications, dielectric materials with stable dielectric permittivity across a large temperature range are highly preferred.

As shown in Figure 4, the relative dielectric permittivities and dielectric loss of pure PI film and F−PI film as a function of frequency in the range from 10^3 to 10^6 Hz at room temperature are presented. The ε_r of the F−PI film is much lower than that of pure PI film. This may be due to the presence of bulky trifluoromethyl groups in F−PI film, giving a marked contribution to decrease the relative dielectric permittivity. Moreover, the ε_r of the films presents the stability with external frequency disturbances. Dielectric loss of both the pure PI and F−PI film is lower than 0.03, which meets the demands of the application in electronic industry.

Thermal Properties of the F−PI Films. In the processing to making ultralarge scale integration (ULSI), there are several processes in high temperature. The main problem is the structural stability of the final porous material. In other words, the collapse of the porous structure must be avoided during the pore-forming process. For this reason, the use of high glass transition temperature polymers is necessary. The TGA results in Figure 5 suggest that the initial decomposition temperature of the SiO_2/PI films with SiO_2 nanoparticle loading at 15 wt % was at 550 °C. We also notice that the porous PI film displays the same thermal decomposition temperature as the SiO_2/PI films. The result confirms that the process to etch SiO_2

dx.doi.org/10.1021/jp305286r | J. Phys. Chem. C 2012, 116, 23676−23681

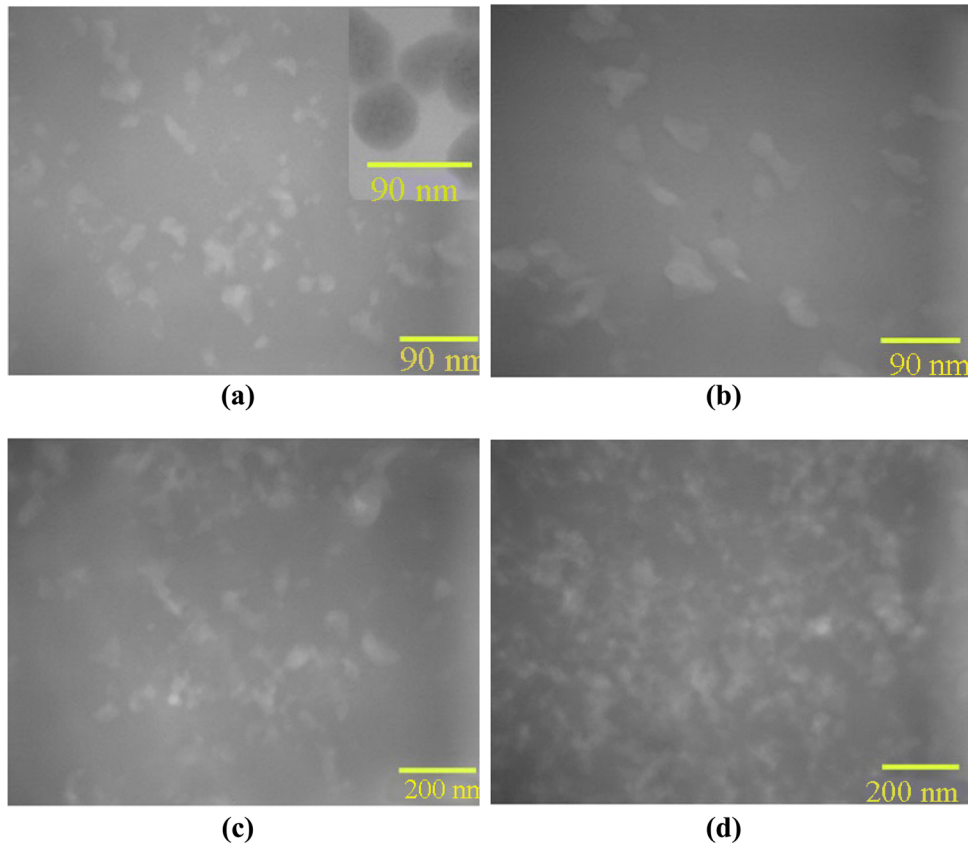

Figure 2. TEM images of the porous F−PI films. Contents of pore-former: (a) 3 wt %; (b) 9 wt %; (c) 12 wt %; (d) 18 wt %. The inset in part a is a TEM image of the SiO_2 nanopaticles.

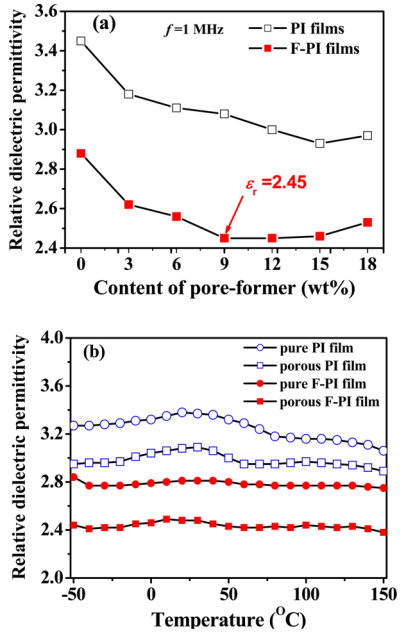

Figure 3. Relative dielectric permittivity dependences on (a) content of the pore-former and (b) temperature in the PI and F−PI films.

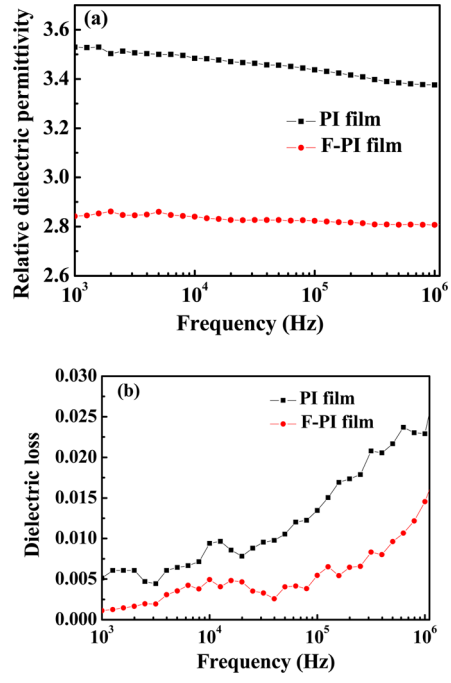

Figure 4. Frequency dependence of (a) relative dielectric permittivity and (b) dielectric loss of pure PI film and F−PI film.

nanoparticles by HF acid does not affect the thermal stability of the PI material. However, as shown in Figure 5, the decomposition temperature of the porous F−PI film is at 480 °C. Therefore, compared to the PI films, thermal stability of the porous F−PI film has exhibited a weak decrease due to the existence of trifluoromethyl groups.

Mechanical Properties of the Porous Films. Water absorption behavior plays an important role in the dielectric

dx.doi.org/10.1021/jp305286r | J. Phys. Chem. C 2012, 116, 23676−23681

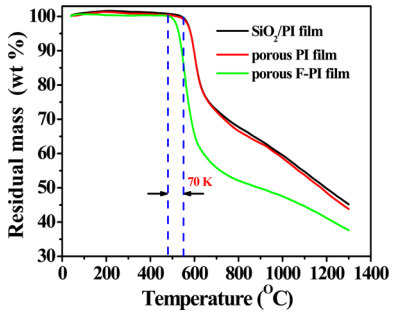

Figure 5. TGA curves of the SiO_2/PI film, porous PI film, and porous F−PI film.

properties of the polymer materials so that this limits their applications in microelectronic industry. Furthermore, water absorption also increases the conductivity of the dielectric materials and may cause corrosion of metal conductors, which can potentially lead to device failure. As shown in Figure 6a, the

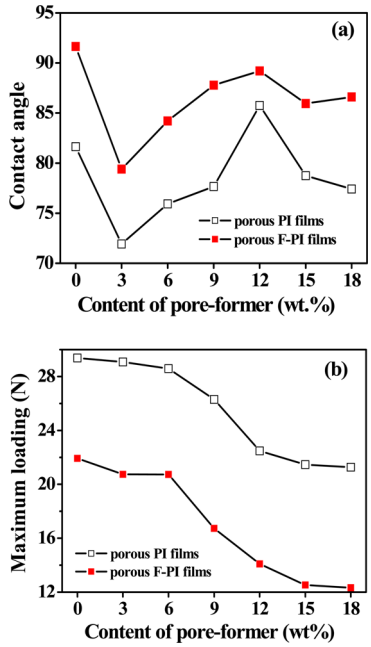

Figure 6. (a) Contact angle and (b) maximum loading dependences on the content of pore-former in the porous PI and porous F−PI films.

contact angles of the porous F−PI films are much bigger than those of the porous PI films. It is clear that the trifluoromethyl groups lead to this difference because of their hydrophobic character. With increasing the content of pore-former, the differences of the contact angles can be attributed to the pore size and porosity of the film.[26] As shown in Figure 6b, the porous F−PI films have a low mechanical strength compared to the porous PI films at different contents of pore former. The F−PI films with a trifluoromethyl group, which is a branched chain structure, can significantly decrease the force between intermolecular chains.[25] When the content of pore-former is below 6 wt %, the size of pores is smaller than 50 nm. In this stage, there is very little decrease in the mechanical strength of the PI films. With increasing pore size and porosity, the mechanical strength of the films decreases significantly.

CONCLUSIONS

In summary, we report an alternative approach to fabricate nanoporous F−PI films with low relative dielectric permittivity, $\varepsilon_r < 2.5$, which is presently the most convenient and simplest method. The SiO_2/F−PI nanohybrid films were first synthesized to employ an in situ polymerization process by controlling the dispersion of SiO_2 nanoparticles in polymer and the chemical reaction of 6FDA and 3FEDAM monomers. Then, the removal of the SiO_2 nanoparticles from the SiO_2/F−PI nanohybrid films by HF acid etching produces nanopores with a diameter of about 40 nm in the F−PI films, which can be confirmed by observing TEM image results. The relative dielectric permittivity of the nanoporous F−PI films was decreased to 2.45, while the films still displayed suitable mechanical properties and thermal stability. These nanoporous F−PI films have a potential application as alternative dielectric layers in the future microelectronic technology.

AUTHOR INFORMATION

Corresponding Author

*E-mail: dangzm@ustb.edu.cn. Phone: +86-10-6233 2599. Fax: +86-10-6233 2599.

Notes

The authors declare no competing financial interest.

ACKNOWLEDGMENTS

This work was financially supported by NSF of China (Nos. 51073015, 50977001, 51207009), the Ministry of Sciences and Technology of China through China-Europe International Incorporation Project (No. 2010DFA51490), State Key Laboratory of Electrical Insulation and Power Equipments (Nos. EIPE12207, EIPE12208), State Key Laboratory of Power System (SKLD11KZ04), China Postdoctoral Science Foundation funded project (No. 20110490291), and the Fundamental Research Funds for the Central Universities (Nos. 06103012, FRF-TP-12-113A).

REFERENCES

(1) Peercy, P. S. *Nature* **2000**, *406*, 1023−1026.
(2) Martin, S. J.; Godschals, J. P.; Mills, M. E.; Shaffer, E. O.; Townsend, P. H. *Adv. Mater.* **2000**, *12*, 1769−1778.
(3) Ree, M.; Yoon, J.; Heo, K. *J. Mater. Chem.* **2006**, *16*, 685−697.
(4) Huang, Y.; Economy, J. *Macromolecules* **2006**, *39*, 1850−1853.
(5) Deligöz, H.; Özgümüş, S.; Yalçınyuva, T.; Yildirim, S.; Değer, D.; Ulutaş, K. *Polymer* **2005**, *46*, 3720−3729.
(6) Liaw, W. C.; Cheng, Y. L.; Liao, Y. S.; Chen, C. S.; Lai, S. M. *Polym. J.* **2011**, *43*, 249−257.
(7) Hougham, G.; Tesero, G.; Viehbeck, A.; Chapple-Sokol, J. D. *Macromolecules* **1994**, *27*, 5964−5971.
(8) Onah, E. J.; Oertel, U.; Froeck, C.; Kratzmuller, T.; Steinert, V.; Bayer, T.; Hartmann, L.; Häußler, L.; Lunkwitz, K. *Macromol. Mater. Eng.* **2002**, *287*, 412−419.
(9) Jang, W.; Shin, D.; Choi, S.; Park, S.; Han, H. *Polymer* **2007**, *48*, 2130−2143.
(10) Paul, A. K. *Annu. Rev. Chem. Biomol. Eng.* **2011**, *2*, 379−401.
(11) Wang, W. C.; Vora, R. H.; Kang, E. T.; Neoh, K. G.; Ong, C. K.; Chen, L. F. *Adv. Mater.* **2004**, *16*, 54−57.
(12) Tseng, M. C.; Liu, Y. L. *Polymer* **2010**, *51*, 5567−5575.
(13) Lee, Y. J.; Huang, J. M.; Kuo, S. W.; Chang, F. C. *Polymer* **2005**, *46*, 10056−10065.
(14) Dang, Z. M.; Yuan, J. K.; Zha, J. W.; Zhou, T.; Li, S. T.; Hu, G. H. *Prog. Mater. Sci.* **2012**, *57*, 660−723.
(15) Simpson, J. O.; Clair, A. K. *Thin Solid Films* **1997**, *308*, 480−485.

(16) Gagliani, J. U.S. Patent 4439381, 1984.
(17) Krause, B.; Koops, G. H.; van der Vegt, N. F. A.; Wessling, M.; Wübbenhorst, M.; van Turnhout, J. *Adv. Mater.* **2002**, *14*, 1041−1046.
(18) Zhao, G. F.; Ishizaka, T.; Kasai, H.; Hasegawa, M.; Furukawa, T.; Nakanishi, H.; Oikawa, H. *Chem. Mater.* **2009**, *21*, 419−424.
(19) Weiser, E. S.; St. Clair, T. L.; Echigo, Y.; Kaneshiro, H. U.S. Patent 6084000, 2000.
(20) Chen, Y. W.; Wang, W. C.; Yu, W. H.; Kang, E. T.; Neoh, K. G.; Vora, R. H.; Ong, C. K.; Chen, L. F. *J. Mater. Chem.* **2004**, *14*, 1406−1412.
(21) Dang, Z. M.; Ma, L. J.; Zha, J. W.; Yao, S. H.; Xie, D.; Chen, Q.; Duan, X. *J. Appl. Phys.* **2009**, *105*, 044104−1−6.
(22) Xu, J.; He, C.; Wei, T. S.; Chung, T. S. *Plast., Rubber Compos.* **2002**, *31*, 295−299.
(23) Fu, G. D.; Shang, Z.; Hong, L.; Kang, E. T.; Neoh, K. G. *Adv. Mater.* **2005**, *17*, 2622−2626.
(24) Deligöz, H.; Yalcinyuva, T.; Özgümüs, S.; Yildirim, S. *Eur. Polym. J.* **2006**, *42*, 1370−1377.
(25) Park, S. J.; Cho, K. S.; Kim, S. H. *J. Colloid Interface Sci.* **2004**, *272*, 384−390.
(26) Chiang, T. H.; Liu, S. L.; Lee, S. Y.; Hsieh, T. E. *Eur. Polym. J.* **2008**, *44*, 3482−3492.